

Investigation of the GeO₂-1,6-Diaminohexane-Water-Pyridine-HF Phase Diagram Leading to the Discovery of Two Novel Layered Germanates with Extra-Large Rings

Bing Guo,^{†,‡,§} Andrew K. Inge,^{‡,§} Charlotte Bonneau,^{‡,||} Junliang Sun,[‡] Kirsten E. Christensen,[§] Zhong-Yong Yuan,[†] and Xiaodong Zou^{*‡}

[†]Institute of New Catalytic Materials Science, College of Chemistry, Nankai University, Tianjin 300071, People's Republic of China, [‡]Inorganic and Structural Chemistry and Berzelii Center EXSELENT on Porous Materials, Department of Materials and Environmental Chemistry, Stockholm University, SE-106 91 Stockholm, Sweden, and [§]Diamond Light Source Ltd., Diamond House, Chilton, Didcot, Oxfordshire, OX11 0DE, United Kingdom. ^{||}Current address: ERATO Kitagawa Integrated Pores Project, Science and Technology Agency (JST), Kyoto Research Park Bldg #3, Shimogyo-ku, Kyoto, 600-8815, Japan, and Institute for Integrated Cell-Material Science (iCeMS), Kyoto University, Yoshida, Sakyo-ku, Kyoto 606-8501, Japan.

Received August 27, 2010

The systematic exploration of the phase diagram of the GeO₂-1,6-diaminohexane-water-pyridine-HF system has allowed the identification of specific roles of the HF, H₂O contents, and HF/H₂O ratio in the formation of Ge₇X₁₉ (Ge₇), Ge₉X_{25–26} (Ge₉), and Ge₁₀X₂₈ (Ge₁₀) clusters (X = O, OH, F). This work has led to the discovery of two novel structures with extra-large 18-membered rings accommodating 1,6-diaminohexane (DAH): SU-63, 11.5H₂DAH-[Ge₇O₁₄X₃]·2H₂O, a layered germanate constructed from Ge₇ clusters with the Kagomé topology, and SU-64, 11H₂DAH[Ge₉O₁₈X₄][Ge₇O₁₄X₃]₆·16H₂O, a germanate built of two-dimensional slabs containing both Ge₇ and Ge₉ clusters (X = OH or F). We also put SU-64 in context with previously reported cluster germanate compounds with related topologies by means of a simple crystal deconstruction study.

Introduction

Oxide materials with uniform pores have been of continuous interest for their potential applications in size and shape selective separation, catalysis, and adsorption.¹ While studies on silica and aluminosilicate systems remain dominant in the field of porous materials, materials based on phosphates²

and germanates³ have caught much interest because of the relative ease of forming structures with extra-large pores (≥ 18-membered rings). To construct such materials, the frameworks often accommodate metals with multiple coordination polyhedra.^{1c} A growing number of germanium oxide based open-frameworks fitting these criteria have been synthesized, as germanium can be four (tetrahedral), five (trigonal bipyramidal or square pyramidal), or six (octahedral) coordinated. The most common cluster building units (CBUs) found in germanate frameworks are the Ge₇X₁₉ (Ge₇),^{4–13} Ge₈X₂₀ (Ge₈),^{13–16} Ge₉X_{25–26} (Ge₉),^{17–20} and Ge₁₀X₂₈ (Ge₁₀)^{21–26} clusters (X = O, OH, F), which always bear negative charges. Except for the Ge₈ cluster which is built of GeO₄ tetrahedra,

*To whom correspondence should be addressed. E-mail: xzou@mmk.su.se.

[†]These authors contributed equally to this work.

(1) (a) Cheetham, A. K.; Ferey, G.; Loiseau, T. *Angew. Chem., Int. Ed.* **1999**, *38*, 3268–3292. (b) *Introduction to Zeolite Science and Practice*, 3rd ed.; Stud. Surf. Sci. Catal.; Čejka, J.; van Bekkum, H., Corma, A., Schüth, F., Eds.; Elsevier: Amsterdam, 2007; Vol. 168. (c) Corma, A. *J. Catal.* **2003**, *216*, 298–312. (d) Sun, J.; Bonneau, C.; Cantin, A.; Corma, A.; Díaz-Cabañas, M. J.; Moliner, M.; Zhang, D.; Li, M.; Zou, X. *Nature* **2009**, *458*, 1154–1157. (e) Davis, M. E. *Nature* **2002**, *417*, 813–821. (f) Schüth, F.; Schmidt, W. *Adv. Mater.* **2002**, *14*, 629–638. (g) Dong, J.; Lin, Y. S.; Kanezashi, M.; Tang, Z. *J. Appl. Phys.* **2008**, *104*, 121301.

(2) (a) Davis, M. E.; Saldarriaga, C.; Montes, C.; Garces, J. M.; Crowder, C. *Nature* **1988**, *331*, 698–699. (b) Jones, R. H.; Thomas, J. M.; Chen, J.; Xu, R.; Huo, Q.; Li, S.; Ma, Z.; Chippindale, A. M. *J. Solid State Chem.* **1993**, *102*, 204–208. (c) Estermann, M.; McCusker, L. B.; Baerlocher, C.; Merrouche, A.; Kessler, H. *Nature* **1991**, *352*, 320–323. (d) Lin, C.-H.; Wang, S.-L.; Li, K.-H. *J. Am. Chem. Soc.* **2001**, *123*, 4649–4650. (e) Yang, G.-Y.; Sevov, S. C. *J. Am. Chem. Soc.* **1999**, *121*, 8389–8390. (f) Khan, I. M.; Meyer, L. M.; Haushalter, R. C.; Schweitzer, A. L.; Zubieta, J.; Dye, J. L. *Chem. Mater.* **1996**, *8*, 43–53. (g) Guillou, N.; Gao, Q.; Forster, P. M.; Chang, J.-S.; Nogués, M.; Park, S.-E.; Ferey, G.; Cheetham, A. K. *Angew. Chem., Int. Ed.* **2001**, *40*, 2831–2834.

(3) (a) Lin, Z.-E.; Yang, G.-Y. *Eur. J. Inorg. Chem.* **2010**, 2895–2902.

(b) Christensen, K. E. *Crystallogr. Rev.* **2010**, *16*, 91–104.

(4) Zhang, H.-X.; Zhang, J.; Zheng, S.-T.; Yang, G.-Y. *Inorg. Chem.* **2003**, *42*, 6595–6597.

(5) Plévert, J.; Gentz, T. M.; Groy, T. L.; O'Keefe, M.; Yaghi, O. M. *Chem. Mater.* **2003**, *15*, 714–718.

(6) Shi, L.; Bonneau, C.; Li, Y.; Sun, J.; Yue, H.; Zou, X. *Cryst. Growth Des.* **2008**, *8*, 3695–3699.

(7) Pan, Q.; Li, J.; Ren, X.; Wang, Z.; Li, G.; Yu, J.; Xu, R. *Chem. Mater.* **2008**, *20*, 370–372.

(8) Pan, Q.; Li, J.; Christensen, K. E.; Bonneau, C.; Ren, X.; Shi, L.; Sun, J.; Zou, X.; Li, G.; Yu, J.; Xu, R. *Angew. Chem., Int. Ed.* **2008**, *47*, 7868–7871.

(9) Li, H.; Eddaoudi, M.; Richardson, D. A.; Yaghi, O. M. *J. Am. Chem. Soc.* **1998**, *120*, 8567–8568.

(10) Plévert, J.; Gentz, T. M.; Laine, A.; Li, H.; Young, V. G.; Yaghi, O. M.; O'Keefe, M. *J. Am. Chem. Soc.* **2001**, *123*, 12706–12707.



Figure 1. Three of the most common clusters in open-framework germanates. (a) The Ge_7 cluster. (b) The Ge_9 cluster. (c) The Ge_{10} cluster. GeO_6 octahedra are in red, GeO_5 trigonal bipyramids in yellow, and GeO_4 tetrahedra in green.

all other clusters comprise germanium atoms with multiple coordination geometries, shown in Figure 1. Among the low-density frameworks are ASU-16^{10,27a} and SU-12^{11,27b} built of Ge_7 and $(\text{Ge}, \text{Si})_7$ clusters, respectively and containing 24-ring channels, and SU-M²¹ built of Ge_{10} clusters and containing 30-ring mesoporous gyroidal channels. The discovery of SU-M²¹ was a promising sign for the further development of cluster compounds with extra-large pores and thus prompted many fruitful studies.^{22,25,28,29} While the majority of reported open-framework germanates consist of only one type of clusters, compounds containing mixed types of clusters could also be made.^{28,29} We found that the same organic template 2-methylpentamethylenediamine (MPMD) in the GeO_2 -MPMD-water-HF system not only resulted in open-framework germanates Ge-pharmacosiderite,²⁴ SU-M,²¹ and SU-61²⁵ with one type of clusters (Ge_{10}), but also yielded open-framework germanates SU-MB,²¹ SU-8,²⁸ and SU-44²⁸ with two types of clusters. SU-MB²¹ is the only example of a structure with both Ge_{10} and Ge_7 clusters. While the framework of SU-MB is the same as SU-M constructed

entirely of Ge_{10} clusters, one of the two gyroidal channels in SU-MB is filled with Ge_7 clusters as “guests”. SU-8, SU-44, and JLG-12^{27c,29} consist of Ge_9 clusters, each of them connects to eight Ge_7 clusters to form a pseudo body-centered cluster aggregate (PBCCA).²⁸

Recently, we reported ASU-21,²² a structure templated by 1,6-diaminohexane with 18-ring channels constructed by rigid packing of hexagonal cylinders of Ge_{10} clusters. As the structure of ASU-21 is very close to a hexagonal polymorph of the cubic SU-M, we decided to undertake a systematic synthetic study to explore a phase diagram against the most important synthesis parameters. We wanted to know whether SU-M could be synthesized in the system and if a transition between the cubic phase SU-M, and the hexagonal phase ASU-21 could be observed in analogy to what was found in mesoporous silica MCM-48 and MCM-41.^{27d,30} While phase diagrams have been established for aluminosilicate³¹ and phosphate³² systems, we are unaware of any such phase diagrams for germanates. Although the anticipated cubic phase SU-M could not be synthesized in our study, the study gave equally important results on tuning synthetic conditions to yield the three different clusters Ge_7 , Ge_9 , and Ge_{10} . The systematic exploration of the GeO_2 -1,6-diaminohexane-water-pyridine-HF system and the resulting phase diagram has allowed us to identify that the HF/ H_2O ratio plays a key role over selective fabrication of the clusters. The study has led to two novel structures with extra-large 18-membered rings: SU-63, a layered germanate constructed of Ge_7 clusters, and SU-64, a two-dimensional slab framework of Ge_7 and Ge_9 clusters with comparable framework topology to ASU-19,⁵ ASU-20,⁵ SU-22,⁶ SU-23,⁶ SU-8, and SU-44.

Experimental Section

Materials. Germanium dioxide (99.99%, Nanjing Chemical Reagent Co.), 1,6-diaminohexane (98%, Sigma-Aldrich), pyridine (99%, Sigma-Aldrich), and hydrofluoric acid (40 wt %, Fluka) were used without further purification. 1,6-Diaminohexane was molten to be measured by volume.

Synthesis. Single crystals of SU-63 suitable for single crystal X-ray diffraction were prepared under solvothermal conditions from a mixture of GeO_2 (312 mg, 2.98 mmol), pyridine (9.00 mL, 111.7 mmol), 1,6-diaminohexane (2.40 mL, 32.6 mmol), and HF (40 wt %, 0.28 mL, 6.4 mmol). The HF 40 wt % included water (0.19 mL, 10.55 mmol). The final molar ratio of GeO_2 : H_2O :Pyridine:DAH:HF is 1:3.5:37.5:10.9:2.2. The mixture was aged for 2 h under constant stirring before being placed in a 22 mL Teflon-lined stainless-steel autoclave and heated at 160 °C under autogenous pressure for 5 days. Colorless crystals of SU-63 with hexagonal plate morphology and on average $150 \times 80 \times 20 \mu\text{m}$ in size were filtered, washed with distilled water, and dried at room temperature overnight.

(30) (a) Huo, Q.; Margolese, D. I.; Stucky, G. D. *Chem. Mater.* **1996**, *8*, 1147–1160. (b) Huo, Q.; Leon, R.; Petroff, P. M.; Stucky, G. D. *Science* **1995**, *268*, 1324–1327. (c) Beck, J. S.; Vartuli, J. C.; Roth, W. J.; Leonowicz, M. E.; Kresge, C. T.; Schmitt, K. D.; Chu, C. T.-W.; Olson, D. H.; Sheppard, E. W.; McCullen, S. B.; Higgins, J. B.; Schlenker, J. L. *J. Am. Chem. Soc.* **1992**, *114*, 10834–10854.

(31) (a) Breck, D. W. *Zeolite Molecular Sieves, Structure, Chemistry, and Use*; Wiley: New York, 1974. (b) Akporiaye, D. E.; Dahl, I. M.; Karlsson, A.; Wendelbo, R. *Angew. Chem., Int. Ed.* **1998**, *37*, 609–611.

(32) (a) Song, Y.; Yu, J.; Li, G.; Li, Y.; Wang, Y.; Xu, R. *Chem. Commun.* **2002**, 1720–1721. (b) Bortun, A. I.; Khainakov, S. A.; Bortun, L. N.; Pojary, D. M.; Rodriguez, J.; Garcia, J. R.; Clearfield, A. *Chem. Mater.* **1997**, *9*, 1805–1811.

(11) Tang, L.; Dadachov, M. S.; Zou, X. *Chem. Mater.* **2005**, *17*, 2530–2536.

(12) Beitone, L.; Loiseau, T.; Férey, G. *Inorg. Chem.* **2002**, *41*, 3962–3966.

(13) Villaescusa, L. A.; Wheatley, P. S.; Morris, R. E.; Lightfoot, P. *Dalton Trans.* **2004**, 820–824.

(14) Li, H.; Yaghi, O. M. *J. Am. Chem. Soc.* **1998**, *120*, 10569–10570.

(15) Conradsson, T.; Dadachov, M. S.; Zou, X. D. *Microporous Mesoporous Mater.* **2000**, *41*, 183–191.

(16) Medina, M. E.; Iglesias, M.; Monge, M. A.; Gutiérrez-Puebla, E. *Chem. Commun.* **2001**, 2548–2549.

(17) Zhou, Y.; Zhu, H.; Chen, Z.; Chen, M.; Xu, Y.; Zhang, H.; Zhao, D. *Angew. Chem.* **2001**, *113*, 2224–2226.

(18) Attfield, M. P.; Al-Ebini, Y.; Pritchard, R. G.; Andrews, E. M.; Charlesworth, R. J.; Hung, W.; Masheder, B. J.; Royal, D. S. *Chem. Mater.* **2007**, *19*, 316–322.

(19) Medina, M. E.; Iglesias, M.; Snejko, N.; Gutiérrez-Puebla, E.; Monge, M. A. *Chem. Mater.* **2004**, *16*, 594–599.

(20) Li, H.; Eddaoudi, M.; Yaghi, O. M. *Angew. Chem., Int. Ed.* **1999**, *38*, 653–655.

(21) Zou, X. D.; Conradsson, T.; Klingstedt, M.; Dadachov, M. S.; O’Keeffe, M. *Nature* **2005**, *437*, 716–719.

(22) Bonneau, C.; Sun, J. L.; Sanchez-Smith, R.; Guo, B.; Zhang, D.; Inge, A. K.; Edén, M.; Zou, X. D. *Inorg. Chem.* **2009**, *48*, 9962–9964.

(23) Medina, M. E.; Gutiérrez-Puebla, E.; Monge, M. A.; Snejko, N. *Chem. Commun.* **2004**, 2868–2869.

(24) (a) Buerger, M. J.; Dollase, W. A.; Garaycochea-Wittke, I. Z. *Kristallogr.* **1967**, *125*, 92–108. (b) Xu, Y.; Cheng, L.; You, W. *Inorg. Chem.* **2006**, *45*, 7705–7708.

(25) Christensen, K. E.; Bonneau, C.; Gustafsson, M.; Shi, L.; Sun, J.; Grins, J.; Jansson, K.; Sbillie, I.; Su, B.-L.; Zou, X. *J. Am. Chem. Soc.* **2008**, *130*, 3758–3759.

(26) Fleet, M. E. *Acta Crystallogr., Sect. C* **1990**, *46*, 1202–1204.

(27) (a) ASU = Arizona State University. (b) SU = Stockholm University. (c) JLG = Jilin University. (d) MCM = Mobile Company Material.

(28) Christensen, K. E.; Shi, L.; Conradsson, T.; Ren, T.; Dadachov, M. S.; Zou, X. D. *J. Am. Chem. Soc.* **2006**, *128*, 14238–14239.

(29) Ren, X.; Li, Y.; Pan, Q.; Yu, J.; Xu, R.; Xu, Y. *J. Am. Chem. Soc.* **2009**, *131*, 14128–14129.

Table 1. Crystallographic Data for SU-63 and SU-64

	SU-63	SU-64
chemical formula ^a	[1.5H ₂ DAH][Ge ₇ O ₁₄ (OH) ₃]·2H ₂ O	[11H ₂ DAH][Ge ₉ O ₁₈ (OH) ₄][Ge ₇ O ₁₄ (OH) ₃]·16H ₂ O
formula weight ^a (g mol ⁻¹)	996.503	7296.846
space group	<i>P6₃cm</i> (185)	<i>P1</i> (2)
<i>a</i> (Å)	28.794(2)	12.101(4)
<i>b</i> (Å)	28.794(2)	18.113(6)
<i>c</i> (Å)	20.603(4)	22.444(8)
α (deg)	90	87.86(1)
β (deg)	90	89.50(2)
γ (deg)	120	83.17(1)
<i>V</i> (Å ³)	14793(3)	4881(3)
<i>Z</i>	6	1
<i>T</i> (K)	100	150
λ (Å)	0.9080	0.6889
ρ _{calcd} (g/cm ³)	1.576	2.238
μ (mm ⁻¹)	6.353	7.817
crystal size (μm)	150 × 80 × 20	30 × 8 × 2
reflections collected	51182	42228
data/restraints/parameters	8692/3/339	15210/11/617
R1 for [<i>I</i> > 2σ(<i>I</i>)] ^b	0.0851	0.1296
wR2 for [<i>I</i> > 2σ(<i>I</i>)] ^c	0.2163	0.3363

^a The formula here includes H₂DAH²⁺ cations and water, which could not be located in the structure refinement but were estimated from elemental analysis. ^b $R1 = \sum ||F_o| - |F_c|| / \sum |F_o|$. ^c $wR2 = [\sum w(F_o^2 - F_c^2)^2 / \sum w(F_o^2)^2]^{1/2}$.

Single crystals of SU-64 were prepared under similar conditions as SU-63 from a mixture of GeO₂ (150 mg, 1.43 mmol), water (1.13 mL, 62.7 mmol), pyridine (4.50 mL, 55.9 mmol), 1,6-diaminohexane (2.10 mL, 28.6 mmol), and HF (40 wt %, 0.08 mL, 1.8 mmol) with a molar ratio of 1:45.7:39.1:20.0:1.3 including water (0.06 mL, 3.3 mmol) present in HF 40 wt %. The mixture was aged for 2 h under constant stirring before being placed in a 22 mL Teflon-lined stainless-steel autoclave and heated at 180 °C for 7 days. Colorless rod-shaped crystals of SU-64 with 30 × 8 × 2 μm in size were separated, washed with distilled water, and dried at room temperature overnight. SU-64 could also be synthesized at 160 °C as was for SU-63; however, the crystals are much smaller than those obtained at 180 °C.

For construction of the phase diagram, crystals of ASU-21,²² SU-63, and SU-64 were prepared from mixtures of GeO₂ (150 mg, 1.43 mmol), pyridine (4.50 mL, 55.9 mmol), 1,6-diaminohexane (2.10 mL, 28.6 mmol), water (0–3.75 mL, 0–208.2 mmol), and HF (0–0.40 mL, 0–9.2 mmol). All samples were heated at 160 °C for 7 days. Products were identified by X-ray powder diffraction (XRPD). Mixtures with even higher water or HF content often resulted in products with poor crystallinity, dense GeO₂, amorphous solid, or no solid recovery.

Characterization. Thermogravimetric (TG) analysis was conducted using a Perkin-Elmer TGA7 on SU-63 and SU-64 under nitrogen atmosphere in a platinum crucible between 20 and 800 °C at a heating rate of 5 °C min⁻¹.

In situ XRPD on SU-63 and SU-64 was performed on a PANalytical X'Pert PRO MRD equipped with an Anton-Parr XRK900 reaction chamber using Cu Kα radiation (λ = 1.5418 Å) and variable slits. The samples were heated under vacuum from room temperature to 500 °C with a heating rate of 7 °C min⁻¹. The temperature was equilibrated for 2 min prior to each measurement. XRPD patterns were first recorded at room temperature, and 50 °C, then up to 200 °C with increments of 50 °C, and finally to 500 °C with measurements every 20 °C. The changes in the unit cell upon heating were examined with JANA2006³³ and PowderCell.³⁴

Elemental analysis of C, H, and N was performed on a Fisons Instruments 1108 at the University of Santiago de Compostela, Spain.

Structure Determination. Single crystal X-ray diffraction data of SU-63 were collected at 100 K on a MarCCD detector using synchrotron radiation (λ = 0.9080 Å for SU-63) at the Beamline I911:5, Max Lab, Sweden. Data reduction and numerical absorption correction were applied with TwinSolve. Single crystal X-ray diffraction data of SU-64 were collected at 150 K on Beamline I19 (EH1), Diamond Light Source, U.K. Diffraction data were collected using a Rigaku CrystalLogic Kappa goniometer with a Saturn 724+ detector at the zirconium absorption edge (λ = 0.6889 Å). Data reduction and numerical absorption correction were applied with d*TREK within CrystalClear.³⁵ The structures were solved by direct methods with SHELXS97.³⁶ All framework atoms were refined with anisotropic displacement parameters for SU-63 and for all germanium atoms in SU-64 using a full-matrix least-squares technique on *F*² with SHELXL97.³⁶ Despite large efforts with many measurements of different crystals, it was not possible to locate the templates in SU-63, presumably because of template disorders. Templates in SU-64 could only be partially located, probably because of the small crystal size (30 × 8 × 2 μm). SQUEEZE was applied using PLATON to manage solvent accessible voids.³⁷ Crystallographic data and refinement details are provided in Table 1. Because of the small crystal size of SU-64, 46% of the reflections were rather weak (with *I* ≤ 2σ(*I*)), resulting in a high R1 value. A more detailed table is provided in the Supporting Information.

Results and Discussion

Crystal Structure Description of SU-63. SU-63 crystallizes in the space group *P6₃cm*. It has a layered structure built solely of Ge₇ clusters (Figure 2a), a cluster building unit with an octahedron coordinated to four tetrahedra in a plane and two trigonal bipyramids bridged by a single tricoordinated oxygen atom (Figure 1a). Each layer contains two symmetry independent Ge₇ clusters forming 6- and 18-membered rings in the *ab*-plane as shown in Figure 2b. SU-63 has two layers in each unit cell, which are related by the *b*₃-axis and are 3.8 Å apart along the *c*-axis.

(35) *CrystalClear*, Version 2.0; Rigaku Corporation: The Woodlands, TX, 2009.

(36) A short history of SHELX: Sheldrick, G. M. *Acta Crystallogr., Sect. A* **2008**, *64*, 112–122.

(37) Spek, A. L. *J. Appl. Crystallogr.* **2003**, *36*, 7–13.

(33) Petricek, V.; Dusek, M.; Palatinus, L. *JANA2006, The crystallographic computing system*; Institute of Physics: Praha, Czech Republic, 2006.

(34) Kraus, W.; Nolze, G. *POWDERCELL*, Version 2.4; Federal Institute for Materials Research and Testing: Berlin, Germany, 1999.

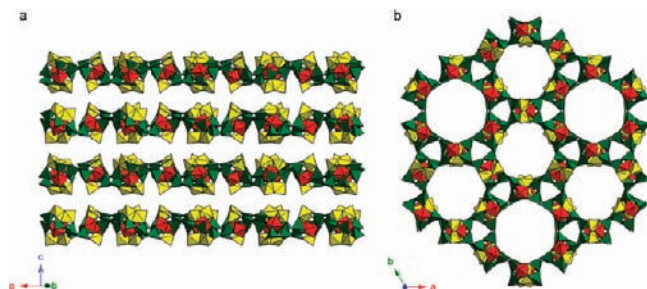


Figure 2. Polyhedral representation of SU-63: (a) Stacking of layers shown along the [120] direction displaying the orientation of the clusters. (b) Projection along the [001] direction showing two types of 18-ring channels running perpendicular to the layers.

The layers stack in such a way that all Ge_7 clusters and the 18-rings overlap with neighboring layers forming one-dimensional channels. All Ge_7 clusters connect to neighboring clusters through their four tetrahedral sites. JLG-4,⁷ ASU-20,⁵ SU-22,⁶ and SU-23⁶ have similar layered structures where the Ge_7 clusters adapt the commonly occurring 4.4.4.4 plane net topology.³⁸ SU-63 is the first layered germanate where cluster building units are arranged in the 3.6.3.6 (Kagomé) plane. It should be noted that this conformation had been primarily ruled out based on a steric hindrance argument.⁵

There are two independent extra-large 18-rings in the structure of SU-63, centered at (0 0 0) (along the 6_3 -axis) and $(1/3, 2/3, 0)$, $(2/3, 1/3, 0)$ (along the 3-fold axes), respectively. The free diameters of the 18-rings are 10.59 and 10.11 Å, respectively. Because of the presence of large pores and the large separation of the layers, the structure has a low framework density of 8.5 Ge atoms per 1000 Å³. The Ge_7 clusters can have two arrangements, as in SU-22 and SU-23, with octahedral sites pointing up or down. All Ge_7 clusters forming the 18-rings around the 6_3 -axis point at the same direction along the c -axis, while the Ge_7 clusters forming the 18-rings around the 3-fold axes point alternatively up and down.

Twenty-seven $\text{H}_2\text{DAH}^{2+}$ ions are expected per unit cell according to the CHN analysis, but no complete $\text{H}_2\text{DAH}^{2+}$ ions could be located presumably because of disorder. Some residual peaks could be located between the layers and form hydrogen-bonds to framework oxygen atoms. However, the electron densities were very low (< 1.5 electron) indicating partial occupancies. The disorder of $\text{H}_2\text{DAH}^{2+}$ ions may be due to the large separation of the layers (3.8 Å) allowing certain freedom of the $\text{H}_2\text{DAH}^{2+}$ orientations. In other related layered structures such as ASU-19, ASU-20, and SU-22, the organic structure directing agents could be located because of the small separation of the neighboring layers (about 2.8 Å) which are hydrogen-bonded to one another.

(38) The point symbol of a node indicates the connectivity of that node to other nodes, indicating the size and sequence of cycles covering all angles. In our study, a Ge cluster represents a node. The 2D topology 4.4.4.4 indicates that each node forms four cycles of size four (4-ring), while a topology of 3.6.3.6 (Kagomé lattice) involves the succession of cycle of size 3 (3-ring), 6 (6-ring), 3 and 6. In topologies containing more than one topological node, the total point symbol indicates the point symbol of each individual node and their relative ratio. For further information, see: Blatov, V. A.; O'Keeffe, M.; Proserpio, D. M. *CrystEngComm* **2010**, *12*, 44–48.

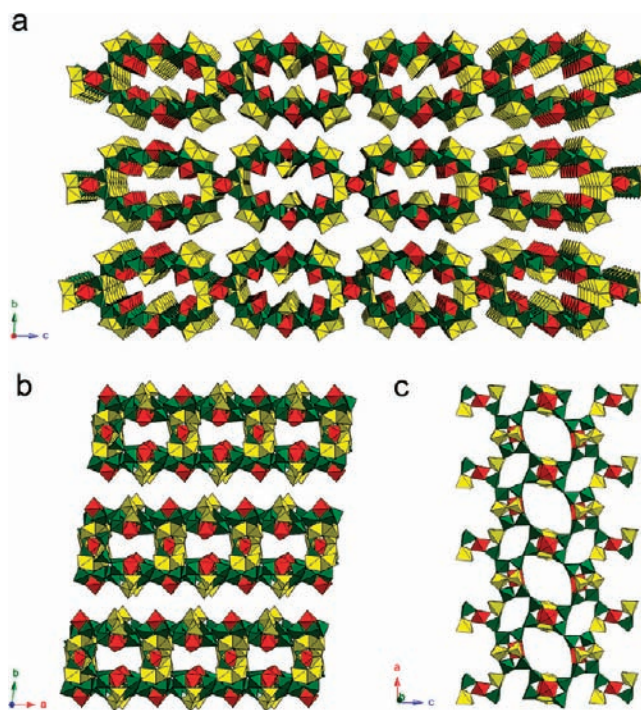


Figure 3. Polyhedral representation of SU-64: (a) 18-ring channels running through the slabs along the [100] direction. (b) 10-ring channels running through the slabs along the [001] direction. (c) A slab in the ac -plane showing the 8- and 12-membered rings.

Crystal Structure Description of SU-64. The structure of SU-64 was solved in space group $P\bar{1}$ and contains not only the four-coordinated Ge_7 cluster as in SU-63 but also the Ge_9 cluster. Each Ge_9 cluster has a central GeO_6 octahedron surrounded by four tetrahedra and four trigonal bipyramids that are available for coordination to a neighboring cluster (Figure 1b). The Ge_9 cluster is generally found to be eight-coordinated. SU-64 has a two-dimensional slab with intersecting 10- and 18-ring channels running through the slab, along the [001] and [100] directions respectively, as shown in Figure 3. The 10-rings are formed by two Ge_9 and two Ge_7 clusters (Figure 3b). The 18-rings are built of six Ge_7 clusters and two Ge_9 clusters at opposite ends of the longest diameter ($\text{O}\cdots\text{O}$ distance of 15.76 Å) (Figure 3a). Each Ge_9 cluster is shared between two neighboring 18-rings. The Ge_9 cluster connects to eight Ge_7 clusters as in SU-8,²⁸ SU-44,²⁸ and JLG-12²⁹ to form a pseudo body-centered cluster aggregate (PBCCA). Two unique Ge_7 clusters each coordinates to two Ge_9 clusters and two Ge_7 clusters, while the third Ge_7 cluster coordinates to four Ge_7 clusters. The Ge_7 and Ge_9 clusters in the layer resemble a 4.4.4.4 net in the ac -plane (Figure 3c), resulting in 8- and 12-ring windows to the 18-ring channels. The framework density of SU-64 is 10.4 Ge atoms per 1000 Å³.

Intercluster hydrogen-bonding was observed in SU-64. Each Ge_7 cluster exhibits hydrogen-bonding ($\text{O}-\text{H}\cdots\text{O}$ distances: 2.72–2.78 Å) to another Ge_7 cluster across the 18-ring channel. The stacking of the slabs along the b -axis is stabilized by hydrogen-bonds between terminal OH/F groups of trigonal bipyramids from the neighboring slabs (Supporting Information Figure S1). The atom types of terminal OH/F groups were indistinguishable by single

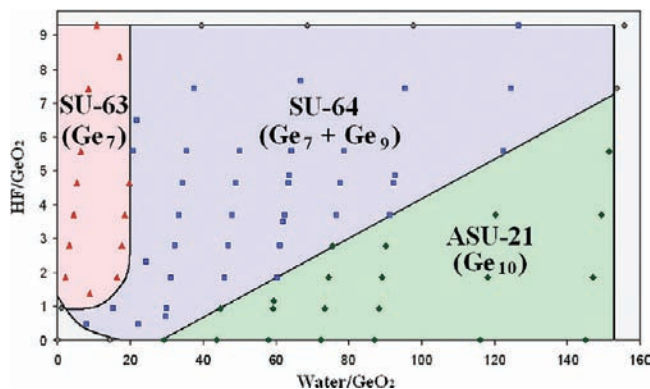


Figure 4. Phase diagram including regions of SU-63 (red), SU-64 (blue), ASU-21 (green), and dense GeO_2 /amorphous material (gray) with quantities of added water and HF (40 wt %) in molar ratios with respect to GeO_2 as variables. Other synthesis parameters are kept the same. Molar ratio: GeO_2 : pyridine: 1,6-diaminohexane = 1: 39.1: 20.0; temperature: 160 °C; synthesis time: 7 days. It should be noted that introducing HF (40 wt %) also increases the amount of water in the system, which has been accounted for and included in the calculation of the water content.

crystal X-ray diffraction because of similar electron densities.

The Ge_9 and Ge_7 clusters have a charge of -4 and -3 , respectively, combining to form a charge of -22 per unit cell. To balance the framework charge, 11 diprotonated $\text{H}_2\text{DAH}^{2+}$ ions are expected in each unit cell, of which five and a half are symmetry-independent. Three of the symmetry-independent $\text{H}_2\text{DAH}^{2+}$ ions could be located crystallographically. One was found inside the slab within the 18-ring channel (Supporting Information Figure S1). One of the amino groups is hydrogen-bonded to three Ge_7 clusters while the other is hydrogen-bonded to two Ge_7 and one Ge_9 clusters. The second $\text{H}_2\text{DAH}^{2+}$ ion was also found inside the slab between two neighboring 18-ring channels, with each of the nitrogen atoms hydrogen-bonded to one Ge_9 and two Ge_7 clusters. The third $\text{H}_2\text{DAH}^{2+}$ ion was found between the neighboring slabs forming hydrogen-bonds to both slabs. Fragments of other $\text{H}_2\text{DAH}^{2+}$ ions could also be located from difference Fourier maps.

Phase Diagram. During the exploratory work around the synthesis conditions of ASU-21,²² the two new phases, SU-63 and SU-64 were found. Structure solutions by single crystal X-ray diffraction revealed that different cluster building units were present in the three different compounds: Ge_7 clusters in SU-63, Ge_7 and Ge_9 clusters in SU-64, and Ge_{10} clusters in ASU-21. It had been observed before that a fluoride media could promote the formation of Ge_7 clusters and the crystallization of compounds regardless of the presence of organic amines.^{4–11,13} The clusters could be found in several structures over a wide range of composition. It was not clear a priori which synthesis parameters direct the formation of the different clusters. Systematic synthesis experiments showed that H_2O and HF were key components for obtaining the different phases, as well as for producing large single crystals. Three domains could be identified as shown in Figure 4.

A relatively high HF and low water content resulted in the formation of SU-63 (Ge_7), while a high water content and absence or low HF content would result in ASU-21 (Ge_{10}). An intermediate quantity of both water and HF

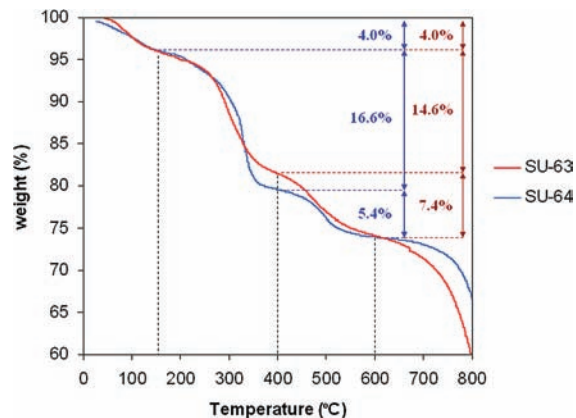


Figure 5. TG traces of SU-63 and SU-64 in nitrogen atmosphere.

produced SU-64 (Ge_7 and Ge_9). We found that when HF was substituted by HCl or H_3PO_4 for the synthesis of SU-63, ASU-21 was formed instead. With very low water and low HF quantities the only recovered solid was dense GeO_2 . With very large amounts of water or HF, only amorphous species were formed. HF is determinant in phase selection, and tends to promote the formation of Ge_7 clusters.^{4–11,13} So far only two reported Ge_7 -containing structures were synthesized without HF, SU-8²⁸ and $\text{Ge}_{10}\text{O}_{21}(\text{OH}) \cdot \text{N}_4\text{C}_6\text{H}_{21}$.¹² The phase boundary between SU-63 and SU-64 is mainly dependent on the $\text{H}_2\text{O}/\text{GeO}_2$ ratio (approximately 20), while that between SU-64 and ASU-21 depends on the $\text{H}_2\text{O}/\text{HF}$ ratio. Mixed phases could be obtained near the phase boundaries.

Characterization. TG analysis was performed to quantify the loss of water and template molecules during thermal treatment. SU-63 and SU-64 showed similar steps of mass losses at similar temperatures. Between 20 and 150 °C, both SU-63 and SU-64 revealed a mass loss of 4.0% (Figure 5), attributed to the loss of crystallographic water molecules indicative of two water molecules per Ge_7 cluster (calculated 3.62%) for SU-63 and 16 water molecules per unit cell for SU-64 (calculated 3.95%). The loss of templates occurred between 200 and 400 °C, with a 14.6% weight loss for SU-63 (calculated 17.8%) and a 16.6% weight loss for SU-64 (calculated 17.8%). Beyond 400 °C, the decomposition of the framework occurs with the loss of terminal OH/F groups between 400 and 600 °C with a mass loss of 7.4% for SU-63 (calculated 6.5%) and 5.4% for SU-64 (calculated 6.6%).

In situ XRPD was performed to study the thermal stability of the crystal structures and changes in unit cell dimensions. As shown in Figure 6a, SU-63 was stable up to 200 °C and decomposed between 200–360 °C when the templates were leaving the structure. During the heating from 30 to 180 °C, $hk0$ peaks were approximately stationary, while all other peaks were shifted to higher 2θ angles, indicating a shortening of the c -axis. From 200 °C, the $hk0$ peaks also started to shift to higher 2θ angles. The unit cell parameters at selected temperatures are given in Table 2. The c -axis was shortened by 1.2 Å from 30–150 °C, indicating that the neighboring layers moved closer to one another by 0.6 Å after the removal of water. The a -axis started to be shorten at 200 °C.

In situ XRPD showed that SU-64 was more stable than SU-63, up to 360 °C (Figure 6b). Peak intensities

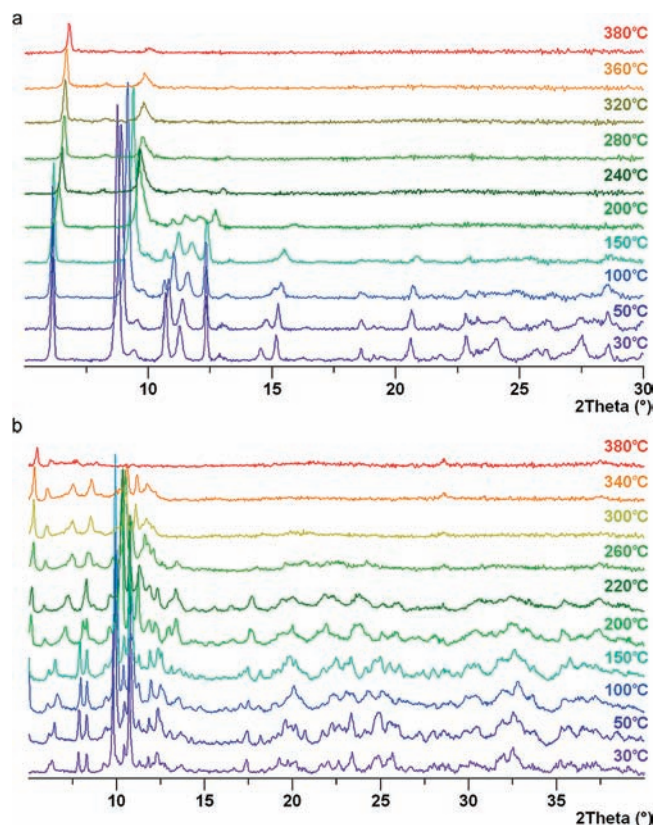


Figure 6. In situ XRPD patterns of (a) SU-63 and (b) SU-64 after background subtraction collected under vacuum.

Table 2. Unit Cell Parameters of SU-63 and SU-64 at Selected Temperatures Determined from in Situ XRPD

temperature (°C)	SU-63		SU-64					
	<i>a</i> (Å)	<i>c</i> (Å)	<i>a</i> (Å)	<i>b</i> (Å)	<i>c</i> (Å)	α (deg)	β (deg)	γ (deg)
30	28.54	20.07	12.18	18.19	22.52	88.21	89.93	82.83
150	28.57	18.87	12.14	18.10	22.35	84.84	90.12	82.01
200	28.03	18.50	11.85	17.67	22.08	79.57	90.89	81.98

decreased significantly after 260 °C when the template molecules began to leave the structure. Predominant peak shifts were observed below 240 °C, with a significant decrease of the α angle (by 9°) from 30 to 200 °C (Table 2). The three unit cell lengths of SU-64 decreased slightly during the heating. This indicates that the neighboring slabs were shifted to one another along the *c*-axis during heating.

Elemental (CHN) analysis showed that the C/N atomic ratio is 3.00 for SU-63 and 3.01 for SU-64, indicating that H₂DAH was the only charge balancing organic species in the crystal structures. The chemical formula can be thus deduced from the crystal structure and CHN analysis as |1.5H₂DAH|[Ge₇O₁₄X₃]·2H₂O for SU-63: observed (wt %): C 11.18, N 4.35, H 3.33, calculated (wt %): C 10.85, N 4.22, H 3.14 and |11H₂DAH|[Ge₉O₁₈X₄][Ge₇O₁₄X₃]₆·16H₂O for SU-64: observed (wt %): C 10.53, N 4.08, H 2.82, calculated (wt %): C 10.86, N 4.22, H 3.18. Calculated values assumed X = OH.

Comparison of Topologies of Germanate Compounds Related to SU-64. From the projections of SU-8,²⁸ SU-44,²⁸ and SU-64, we can see that the compounds

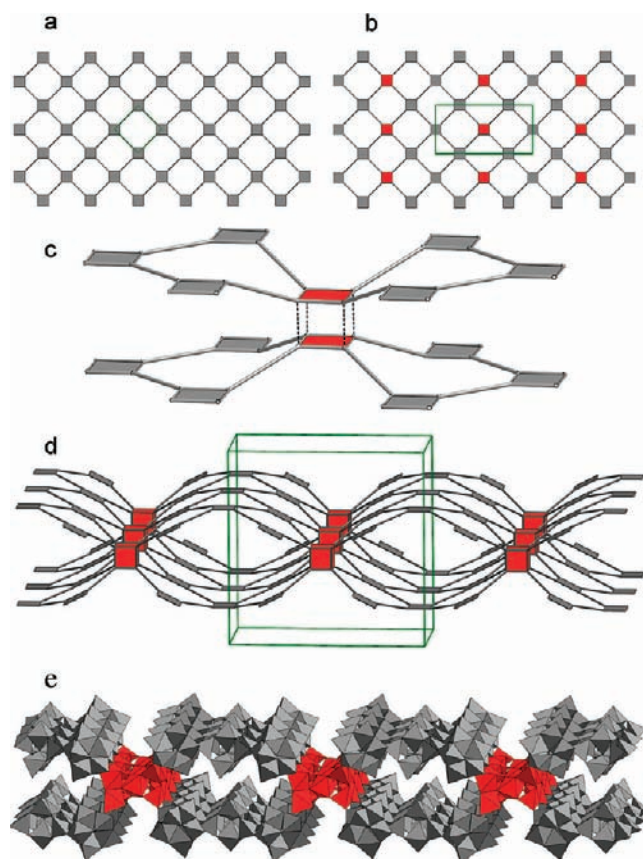


Figure 7. Construction of the SU-64 topology from the 4.4.4.4 net. Vertices are represented in their augmented version, that is, the vertices are represented by their coordination polyhedra. (a) sq1 net with gray squares representing four-coordinated nodes; (b) the new colored net in *pmm*, squares in red indicating those to be fused to create eight-coordinated nodes; (c) fusing the red squares; (d) the resulting topology; (e) polyhedral representation of the slab in SU-64.

have a common motif based on a 4.4.4.4 topology,³⁸ as has already been identified several times in 2D layered compounds.^{5,6} The highest symmetry of the 4.4.4.4 topology corresponds to a square layer: *p4m* with a square unit cell (Figure 7a). If we color every fourth vertex of the plane net in red, the symmetry is reduced to *pmm*, and the cell is now rectangular (Figure 7b). Stacking the layers eclipsed and fusing the red vertices between a pair of layers produces eight-coordinated “red” vertices (Figure 7c), and a double layer slab is formed with topology {4¹⁶.6¹²}{4⁴.6²}₆ (Figure 7d).³⁸ If we now decorate the gray vertices with Ge₇ clusters and the red vertices with Ge₉ clusters, we find the slab of SU-64.

The connectivity of clusters in mixed Ge₇ and Ge₉ frameworks SU-8, SU-44, and JLG-12²⁹ may also be described in a similar manner. SU-44 exhibits similar slabs as in SU-64, with the addition of non-cluster tetrahedra that bridge the layers resulting in a three-dimensional framework (Figure 8c). The plane net projection (Figure 8a) includes two blue vertices indicating Ge₇ clusters bridged by GeO₄ tetrahedra; in details the blue vertices become six-coordinated and the overall topology is that of a three nodal net (Figure 8b).³⁹ Coming back to the uncolored sq1 net, if now every second vertex in the

(39) The SU-44 topology embedding with details of the coordination sequence and point symbols is provided in the Supporting Information.

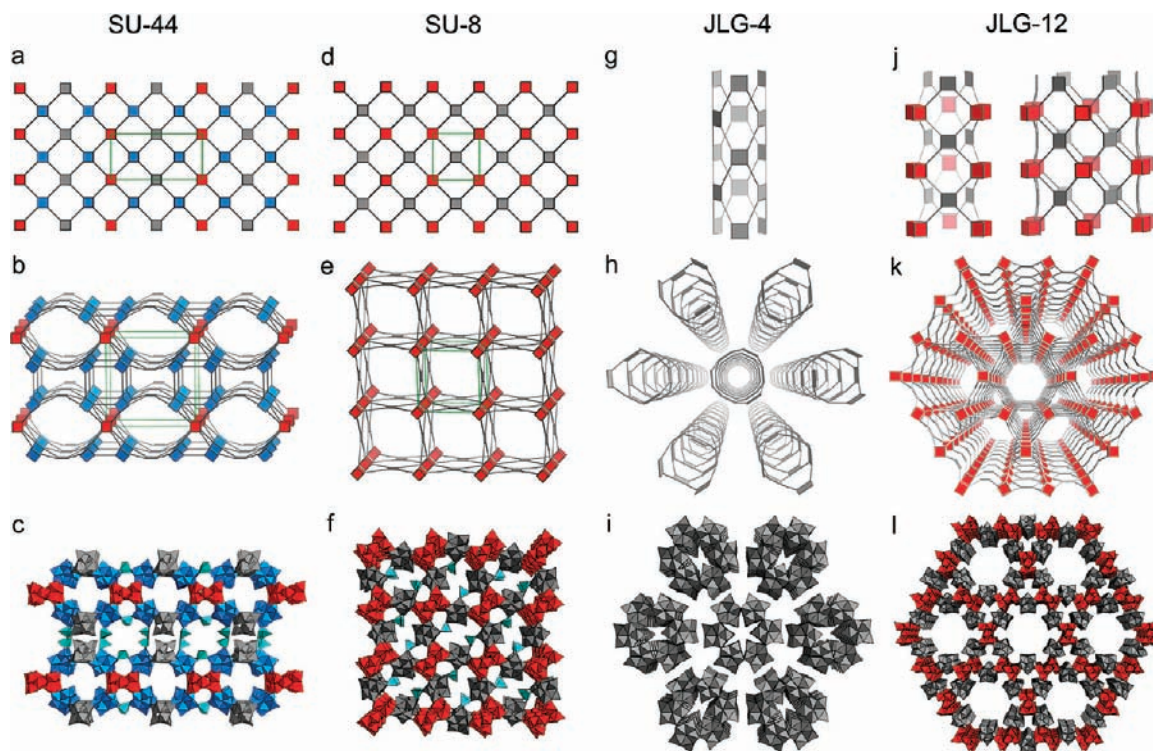


Figure 8. Augmented representations of the nets corresponding to SU-44, SU-8, JLG-4, and JLG-12 based on the 4.4.4.4 net. Top: plane net projections of SU-44 and SU-8, and the **sql** net rolled into cylinders in JLG-4 and JLG-12. Center: three-dimensional nets of SU-44, SU-8, and JLG-12, and hexagonal packing of cylinders in JLG-4. Bottom: polyhedral representations of SU-44, SU-8, JLG-4, and JLG-12. Ge_9 clusters are shown in red and Ge_7 clusters in gray and blue.

square net is replaced by red vertices, a new square cell is defined while keeping the $p4m$ symmetry (Figure 8d); this can be thought as being a binary version of the **sql** net. Stacking these layers by making the red vertices fused to become eight-coordinated, we obtain a three-dimensional net (**scu**) (Figure 8e) corresponding to SU-8 (Figure 8f); note that in the 3D high symmetry group, the squares now lie in planes orthogonal to each other. What has been described for plane figures can also be done for cylindrical objects. **sql** can be wrapped onto cylinders of different diameters. JLG-4 (Figure 8i),⁷ for example, is a tubular structure of Ge_7 clusters wrapped onto a cylinder (Figures 8g and 8h). The cylinder has with a “perimeter” of six squares corresponding to six Ge_7 clusters. Such a square tiling of a cylinder corresponds to the only cylindrical topology exhibiting one kind of edge.⁴⁰ If we now color one out of two squares (three alternative red and gray squares, Figure 8j left) and glue the red vertices together, we obtain the three-dimensional **csq** net (Figure 8k), which has recently been reported in the germanate JLG-12 (Figure 8l).²⁹ Alternatively the **csq** net can be constructed from twelve square perimeter cylinders (Figure 8j right) with alternating gray and red squares.

(40) Eddaoudi, M.; Kim, J.; Vodak, D.; Sudik, A.; Wachter, J.; O’Keeffe, M.; Yaghi, O. M. *Proc. Natl. Acad. Sci. U.S.A.* **2002**, *99*, 4900–4904.

Conclusions

We have presented an extensive synthesis study on the GeO_2 -1,6-diaminohexane-water-HF system leading to the first phase diagram for an open-framework germanate system. By tuning the quantity of water and HF in the reaction mixture, we have introduced various cluster building units in the frameworks, which led to the discovery of two novel germanate structures with extra-large 18-membered rings. We believe that the establishment of ties between synthesis conditions and the resulting structures is of importance to the discovery of other novel open-frameworks.

Acknowledgment. This project is supported by the Swedish Research Council (VR) and the Swedish Governmental Agency for Innovation Systems (VINNOVA) through the Berzelii Center EXSELENT. We thank Max Peskov for the initial topology analysis of SU-63 and SU-64 and valuable discussions. C.B. and J.-L.S. were funded by grants from the Wenner-Gren and Carl-Trygger Foundations, respectively.

Supporting Information Available: Crystallographic data for SU-63 and SU-64 and the corresponding CIF files, the structure of SU-64 showing the location of $\text{H}_2\text{DAH}^{2+}$ cations and selected hydrogen-bonds, and the topology embedding Systre file of SU-64 in CGD format. This material is available free of charge via the Internet at <http://pubs.acs.org>.